



## Architectural influence of carbazole *push–pull–pull* dyes on dye sensitized solar cells



Ashok Keerthi<sup>a,b</sup>, Deepa Sriramulu<sup>a</sup>, Yeru Liu<sup>b,c</sup>, Chan Thuang Yuan Timothy<sup>a</sup>, Qing Wang<sup>b,c,1</sup>, Suresh Valiyaveetil<sup>a,b,\*</sup>

<sup>a</sup> Department of Chemistry, National University of Singapore, 3 Science Drive 3, Singapore 117543

<sup>b</sup> NanoCore-NUSNNI, T-Lab Building, National University of Singapore, 5A Engineering Drive 1, Singapore 117411

<sup>c</sup> Department of Materials Science and Engineering, Faculty of Engineering, National University of Singapore, Singapore 117574

### ARTICLE INFO

#### Article history:

Received 22 May 2013

Received in revised form

1 July 2013

Accepted 3 July 2013

Available online 13 July 2013

#### Keywords:

Dye sensitized solar cells

Organic dyes

Carbazole dyes

Donor–acceptor

Frontier orbitals

HOMO–LUMO

Cyclic voltammetry

### ABSTRACT

Herein we report design, synthesis, characterization and application of a series of molecules with D- $\pi$ -A structures that contain a *push–pull–pull* with substituted carbazole as the electron donor and cyanoacrylic acid as the electron acceptor bridged by a benzothiadiazole fragment. Theoretical, electrochemical and photophysical properties of the target molecules with respect to the chemical nature and position of substituent on the carbazole moiety were investigated in detail. The substituents on carbazole changed the solubility, packing and orientation of molecules on the TiO<sub>2</sub> surface of DSSCs. The dye sensitized solar cell performances of the molecules were studied and compared with respect to the position and substituent.

© 2013 Elsevier Ltd. All rights reserved.

## 1. Introduction

In recent years, quest for renewable energy has received worldwide attention owing to the fast depletion of fossil fuel reserves and environmental pollution problems accompanying fossil fuel consumption. Solar energy conversion devices that convert sunlight into electricity are seen as inevitable future energy candidates due to the unlimited supply of solar energy [1,2]. Inorganic silicon based solar cell technology has shown 30–40% conversion efficiency [3], which is the highest so far. However, silicon based devices are expensive with respect to cost and availability. Therefore the low-cost alternatives based on organic materials, such as organic dye-sensitized solar cells (DSSCs) are potential alternatives to develop an environmentally viable and cost effective technology [4–10].

Most successful metal complexes of organic molecules employed so far in DSSC were ruthenium based metal complexes, which yielded an overall conversion efficiency of up to 11% under AM1.5 irradiation [2,11–13]. However, ruthenium dyes are very expensive and metal free sensitizers such as organic dyes and natural dyes are being investigated as alternative sensitizers for DSSC applications [14,15]. Recent literature reports indicate achievement of highest efficiency up to 12% using organic dyes [16–18]. Several organic dyes based on coumarins [19,20], porphyrin [10,21,22], indoline [23] and cyanine [24] with varying degree of efficiency have been reported in the literature.

Organic dyes provide structural versatility to tune the absorption wavelength, molar extinction coefficient, and HOMO–LUMO energy levels [25,26]. The donor-( $\pi$ -spacer)-acceptor system has been used for designing organic sensitizers due to their effective photo-induced intramolecular charge transfer characteristics [15,17,27,28]. Dyes with strong light-absorbing capability in the red and near IR region, photo stability and redox stability are presumed to be attractive for fabricating stable DSSCs [7].

Carbazole molecule has been widely used as a functional building block or substituent for the preparation of organic photoconductors, non-linear optic (NLO) materials, hole-transport materials, efficient dyes for solar cells, organic light-emitting devices (OLED) and as host materials for phosphorescence

\* Corresponding author. Department of Chemistry, National University of Singapore, S5-01-01, Materials Research Laboratory, 3 Science Drive 3, Singapore 117543. Tel.: +65 65164327; fax: +65 67791691.

E-mail addresses: [msewq@nus.edu.sg](mailto:msewq@nus.edu.sg) (Q. Wang), [chmsv@nus.edu.sg](mailto:chmsv@nus.edu.sg) (S. Valiyaveetil).

<sup>1</sup> Department of Materials Science and Engineering, National University of Singapore, Blk. E2, #05-27, 5 Engineering Drive 2, Singapore 117576. Tel.: +65 6516 7118; fax: +65 6776 3604.

applications [7,28–30]. Moreover, thermal stability and glassy state durability of organic molecules were found to be significantly improved upon incorporation of a carbazole moiety in the structure [31]. Benzothiadiazole based polymers have been widely employed in photovoltaic applications [32]. Benzo(thia/selena)diazole based fluorophores with low-lying excited state showed low-energy absorption based on charge transfer, charge separation and migration processes [33,34].

Koumura et al., have studied extensively on carbazole based dyes in DSSCs by varying  $\pi$ -conjugated bridge and alkyl chain substitution effects [8,29,35–37]. In this article, design, synthesis, characterization and application of six organic dyes that contain carbazole derivatives as the electron donors and cyanoacrylic acid as the electron acceptor bridged by an electron deficient benzothiadiazole fragment to form a *push-pull-pull* model, are reported (Fig. 1). Such systems demonstrate that low-band gap chromophores do function as a photon sinks where charge separation is facilitated by the presence of donor and acceptor units. By linking carbazole's 2nd or 3rd positions to the benzothiadiazole group and changing the functional groups on the N-atom of carbazole, we hope to investigate subtle role of changes in conformation, electronic energy levels, solubility and self-assembly of the target molecules in photophysical and energy conversion efficiencies.

## 2. Results and discussion

### 2.1. Synthesis and characterization

The dyes were obtained in three steps as illustrated in Schemes 1 and 2. In the first step, the substituted carbazole is attached to the

dibromobenzothiadiazole by Suzuki coupling reactions. These reactions also produced disubstituted side products, however, the monosubstituted compounds can be separated using column chromatography in good yield. In the next step, 5-formyl thiophene-2-boronic acid was attached to monocapped benzothiadiazole compounds by Suzuki coupling to produce corresponding aldehydes. These aldehydes react with cyanoacetic acid in the presence of piperidine in chloroform to produce the target molecules, which appeared as dark brown powder.

The solubility of all synthesized dyes was checked in chloroform, tetrahydrofuran (THF) and dimethylsulfoxide (DMSO). **SD1** showed poor solubility in chloroform ( $\sim 1$  mg/mL), partial solubility in tetrahydrofuran ( $\sim 2$  mg/mL) and molecular aggregation. **SD1** dissolves in polar solvents such as DMSO ( $\sim 4$  mg/mL). **SD2** and **SD5** showed partial solubility in chloroform ( $\sim 2$  mg/mL), but moderately soluble in THF (3 mg/mL) and DMSO (6 mg/mL). The dyes **SD4** and **SD6** showed moderate to good solubility in chloroform (3 mg/mL), THF (4 mg/mL) and DMSO (8 mg/mL) due to the presence of solubilizing groups on the carbazole unit. **SD3** showed relatively high solubility in chloroform (6 mg/mL), THF ( $\sim 10$  mg/mL) and DMSO ( $\sim 15$  mg/mL) among the other dyes.

Thermogravimetric analysis (TGA) and differential scanning calorimetry were performed (Figure S6) to investigate the thermal stability and melting points of the target molecules. All compounds exhibit thermal stability under nitrogen atmosphere with a decomposition temperature in the range of 150–220 °C (weight loss, 5%). Differential scanning calorimetry (DSC) measurements showed the glass transition ( $T_g$ ) temperatures at 104, 112 and 108 °C for **SD2**, **SD3** and **SD6**. FT-IR spectra of all compounds (see Supporting information) showed characteristic absorption peaks at

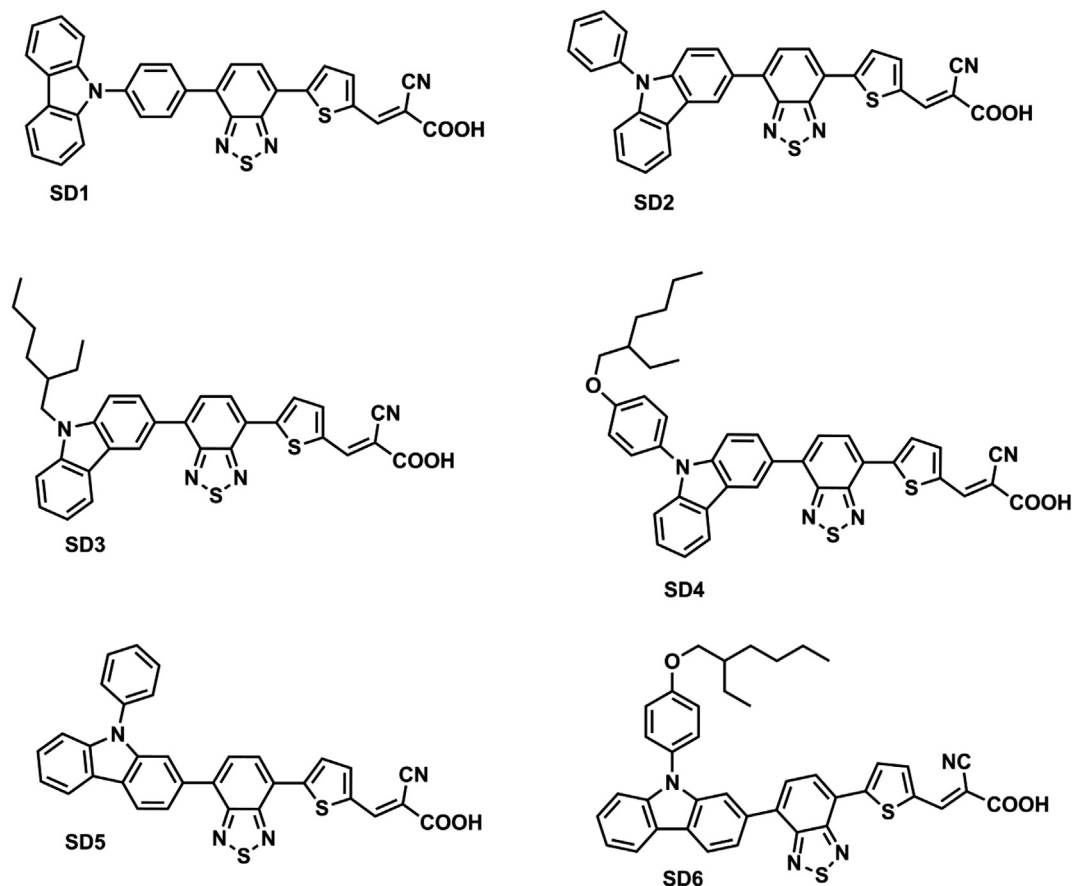
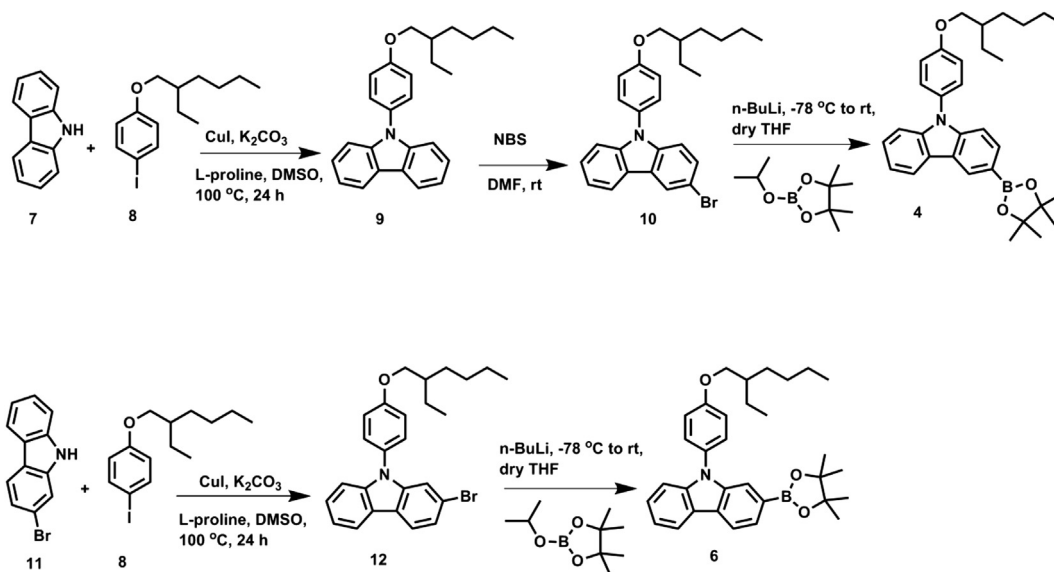


Fig. 1. Chemical structures of synthesized carbazole dye molecules.



**Scheme 1.** Synthesis of [9-(3-carbazol- boronic ester)-phenyl-4-hexyloxy] (**4**) and [9-(2-carbazol-boronic ester)-phenyl-4-hexyloxy] (**6**).

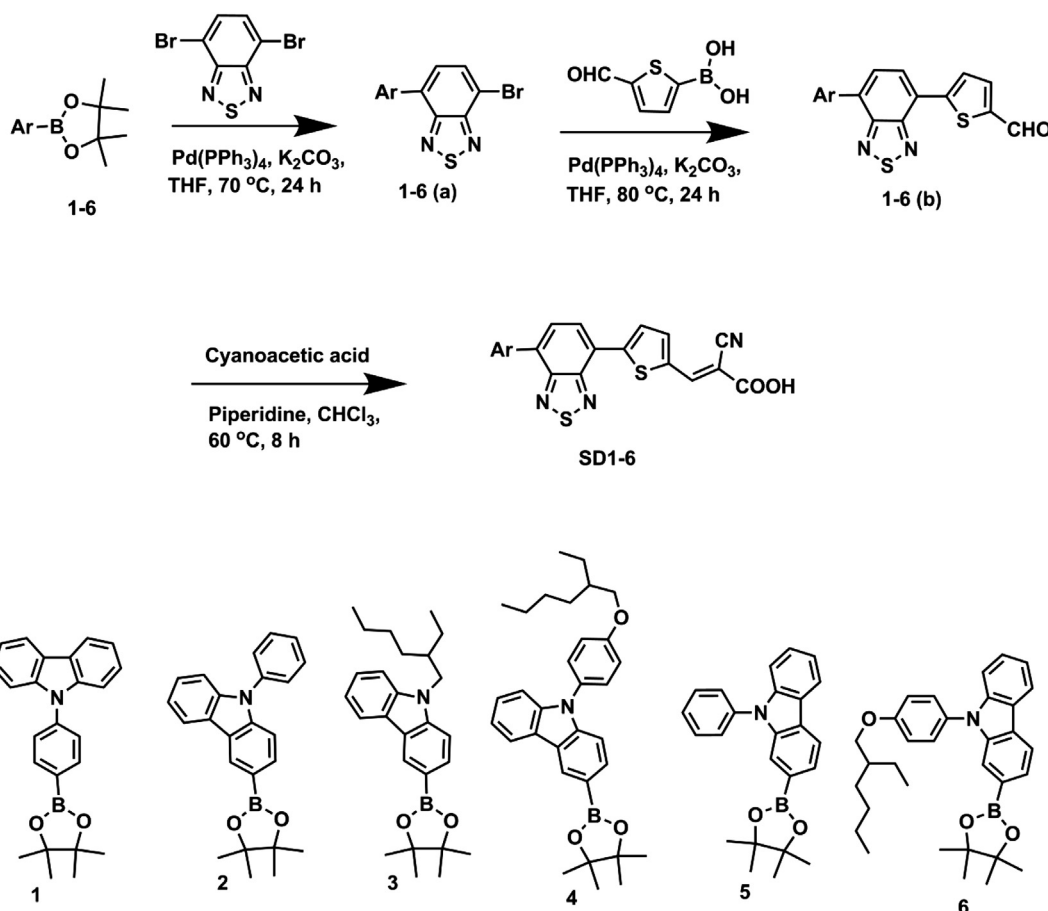
$3430\text{ cm}^{-1}$  (OH stretching);  $1650\text{--}1680\text{ cm}^{-1}$  (C=O stretching) and  $2214\text{ cm}^{-1}$  (CN stretching).

## 2.2. Photophysical properties

Normalized absorption and emission spectra of all six compounds (**SD1–6**) in THF solution are shown in Fig. 2 (A and C). Compound **SD1**

shows absorption peak at 445 nm. It is observed that carbazole connected through N-phenyl ring to the benzothiadiazole in a D- $\pi$ -A fashion are rotated by  $\sim 60^\circ$  and  $\sim 36^\circ$  angles from geometry optimized structures. This break in planarity and conjugation would cause the blue shift in absorption peak compared to compounds **SD2–6**.

Compounds **SD2–SD6** showed two absorption bands around 370 nm and 470 nm. The absorption peak around 370 nm is due to



**Scheme 2.** General synthetic reaction scheme for dyes, **SD1–SD6**.

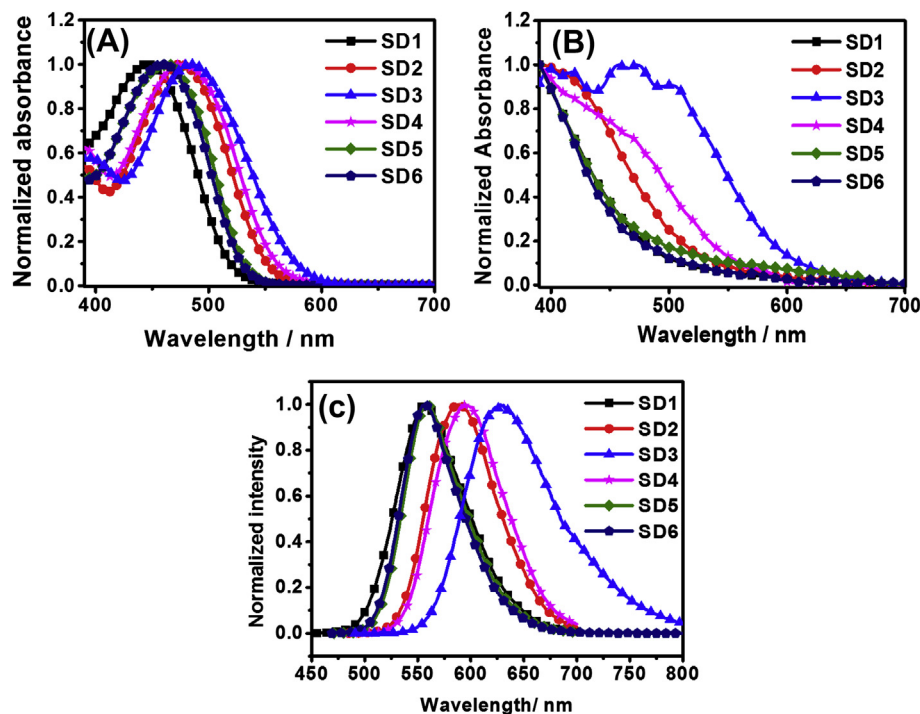


Fig. 2. Normalized UV–visible absorption spectra of dyes in solution state (A), on TiO<sub>2</sub> thin film (B) and emission spectra (C) in THF at room temperature.

$\pi$ – $\pi^*$  electronic transition of conjugated molecule and the peak around 470 nm is due to intramolecular charge transfer between the donor and acceptor moieties. **SD2** and **SD4** showed a redshift in absorption maxima (474–476 nm) by 15–20 nm as compared to **SD5** and **SD6** (461 nm–459 nm) due to linkage of benzothiadiazole on 3-position of carbazole donor unit. Similarly, linking benzothiadiazole at 2-position of carbazole donor unit as in **SD5** and **SD6**, led to decrease of conjugation extension and reduction in the charge transfer from donor to the acceptor. The same trend was observed in the case of molar absorption coefficients of the dyes (Table 1). The above differences in absorption maxima are observed due to the acceptor moiety on 3-position of N-phenyl carbazole which is rich in electron density and increases  $\pi$ -conjugation effect compared to 2-position of N-phenyl carbazole. The absorption spectra of dye-adsorbed TiO<sub>2</sub> films were measured (Fig. 2B) and except for **SD3**, they were in good agreement with solution state absorption spectra. **SD3** showed broad absorption spectrum compared to other dyes. As expected, the onset absorption wavelengths of dye-adsorbed TiO<sub>2</sub> films were red shifted compared to solution state absorption of dyes.

### 2.3. Electrochemical properties

For efficient electron injection, the lowest unoccupied molecular orbital (LUMO) or excited state redox potential of the dye should be

above the conduction band edge of TiO<sub>2</sub>. Similarly for efficient dye regeneration, the highest occupied molecular orbital (HOMO) of the dye should lie below the energy level of redox ( $I^-/I_3^-$ ) system [38]. To evaluate the thermodynamic basis of these electron transfer processes, cyclic voltammetry (CV) was used to assess the energy levels of the sensitizers. Cyclic voltammograms for all molecules are shown in Fig. 3 and the corresponding parameters are given in Table 1. The molecules are electrochemically stable and exhibit quasi-reversible oxidation and reduction couples.

The HOMO and LUMO levels of all dye molecules were found to be similar due to the same acceptor and anchoring groups. For higher performance, the HOMO potential of the molecule should be sufficiently positive compared to the redox potential of electrolyte for efficient dye regeneration. The LUMO levels of all dyes are at higher energy level than the conduction band edge energy level ( $E_{cb}$ ) of TiO<sub>2</sub> (–4.4 eV), which implies that electron injection from the excited dye into the conduction band (CB) of TiO<sub>2</sub> is feasible. The molecules absorb light upon illumination and electrons in HOMO levels get excited to LUMO levels and transfer electrons to the conduction band of TiO<sub>2</sub>.

### 2.4. Theoretical calculations

The Gaussian calculations were carried out on Gaussian 09 at the density functional theory (DFT) level with the B3LYP function

Table 1  
Summary of photophysical and electrochemical properties of carbazole dyes.

Dye	$\lambda_{abs}^a$ (nm)	Molar absorption coefficient, $\epsilon$ (mol <sup>-1</sup> dm <sup>3</sup> m <sup>-1</sup> )	$\lambda_{em}^a$ (nm)	$E_{oxid}^b$ (V)	$E_{red}^b$ (V)	HOMO (eV)	LUMO (eV)	$E_g$ (eV)
<b>SD1</b>	445	23,993	557	0.48	–1.33	–5.28	–3.47	1.81
<b>SD2</b>	474	25,712	589	0.49, 0.81	–1.34	–5.29	–3.46	1.83
<b>SD3</b>	484	26,206	628	0.44, 0.69	–1.26, –1.80	–5.24	–3.54	1.70
<b>SD4</b>	476	26,107	595	0.67	–1.35, –1.75	–5.47	–3.45	2.02
<b>SD5</b>	459	10,239	560	0.50	–1.33	–5.30	–3.47	1.83
<b>SD6</b>	461	11,021	557	0.61, 0.83	–1.36, –1.72	–5.41	–3.44	1.97

[a] Recorded in THF. [b] vs ferrocene in 0.1 M Bu<sub>4</sub>NPF<sub>6</sub> in THF with platinum disc as working electrode with a scan rate of 100 mV s<sup>-1</sup>.

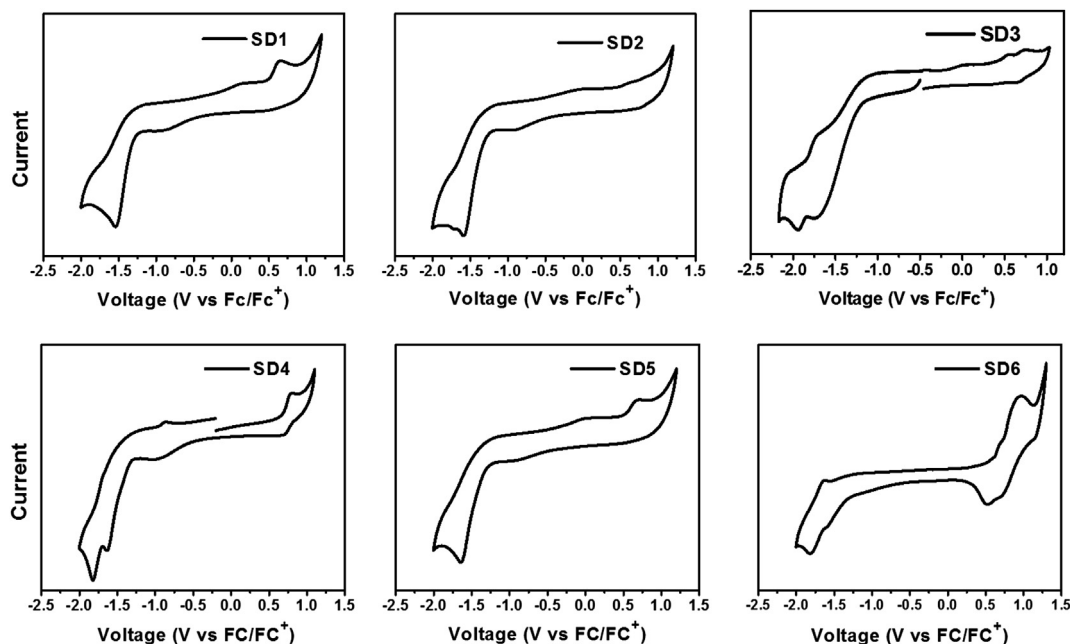


Fig. 3. Cyclic voltammetry scans of dyes **SD1–SD6** at a scan rate 100 mV/s.

using 6-31G\* as a basis set. The geometry optimized structures (see Supporting information) and frontier orbital energy levels were calculated. The HOMO/LUMO orbital distributions of carbazole substituted benzothiadiazole molecules were calculated (Fig. 4). The dihedral angles ( $\alpha$ ) between carbazole connectivity ring and benzothiadiazole were calculated and summarized in Table 2.

The simulated HOMO–LUMO levels and trends in band gaps of the dye molecules were in agreement with UV–vis absorption spectra of the dyes. The frontier molecular orbital distributions of the dyes were different for dyes connected to benzothiadiazole via 2nd or 3rd position of the carbazole. In case of dyes **SD2**, **SD3** and **SD4**, the HOMO levels were fully distributed on the whole molecule whereas the LUMO levels were localised in between benzothiadiazole and cyanoacrylic acid groups. The HOMO levels of dyes **SD1**, **SD5** and **SD6** were mostly localized on carbazole moiety, however, the LUMO levels are on acceptor moieties. There is no much significant difference found in the dihedral angle between benzothiadiazole and carbazole linkage.

### 2.5. Photovoltaic performances of DSSCs

The photovoltaic performances of these dyes were evaluated by constructing DSSC in conjugation with nanocrystalline TiO<sub>2</sub> and the (I<sup>-</sup>/I<sub>3</sub><sup>-</sup>) redox system. Photocurrent spectra of **SD1–SD6** based DSSCs are shown in Fig. 5A, where the monochromatic incident photons to photocurrent conversion efficiencies (IPCEs) are plotted as a function of wavelength. Current–voltage characteristics of these DSSCs are shown in Fig. 5B. IPCE spectra of **SD1–SD4** are broad and red shifted by 40 nm as compared to **SD5** and **SD6**. The maximum IPCE for **SD2** showed about 44% at 450 nm, **SD1** reached about 40% at 460 nm while **SD3** and **SD4** showed about 35% at 450 nm. All four dyes (**SD1–SD4**) showed higher photocurrent compared to **SD5** and **SD6**, which is consistent with the IPCE spectra (Fig. 5A). The IPCE spectra of dyes **SD5** and **SD6** exhibited much lower IPCE of 25% at 440 nm and 16% at 429 nm respectively, which is reflected in lower photocurrent and hence low photovoltaic performances. Surprisingly, **SD3** showed broad photocurrent spectrum compared to **SD2** and **SD4**, which is also

supported by UV–vis absorption spectra of dyes in solution and on TiO<sub>2</sub> film (Fig. 2A and B). The IPCE spectra of all the dyes are in well agreement with UV–vis absorption spectra of dye-adsorbed TiO<sub>2</sub> films.

The photovoltaic parameters of **SD1–SD6** were summarised in Table 3. The overall conversion efficiency ( $\eta$ ) is calculated from the short circuit current ( $J_{SC}$ ), open circuit voltage ( $V_{oc}$ ) and fill factor (FF).

As tabulated in Table 3, **SD3** showed highest efficiency among the six dye molecules. The overall power conversion efficiency ( $\eta$ ) of these molecules were in the order of **SD3** > **SD2** > **SD4** > **SD1** > **SD5** > **SD6**, respectively. **SD1** showed significantly low efficiency compared to triphenylamine containing equivalent dye [39]. This could be due to low solubility and dye aggregation of carbazole dye on TiO<sub>2</sub> surface. **SD5** and **SD6** showed poor power conversion efficiency with low short circuit current. This may be due to the linking of benzothiadiazole acceptor to the 2-position of carbazole moiety with a reduction in  $\pi$ -conjugation. In case of dyes **SD2–SD4**, the benzothiadiazole is linked to 3-position of the carbazole group which showed higher power conversion efficiencies. These results emphasize the importance of  $\pi$ -conjugation in achieving high power conversion efficiency.

The slightly larger short circuit current ( $J_{SC}$ ) of **SD2–SD4** over **SD1** may be attributed to relatively easy electron transfer from the carbazole group to the acceptor moiety. Alkoxy substituted **SD4** and **SD6** showed low short-circuit current and poor conversion efficiency than **SD2** and **SD5**, respectively. This might be due to slower regeneration kinetics of dyes **SD4** and **SD6** with bulky 4-phenylalkoxy substituent on carbazole [40]. The power conversion efficiency of 2-ethylhexyl substituted **SD3** is higher than the phenyl or phenylalkoxy substituted **SD2** or **SD4**, which supports the hypothesis that dye regeneration by the I<sup>-</sup> is slower for dyes with more bulky substituents. All the dyes showed moderate power conversion efficiencies, which might be due to the dye aggregation and intermolecular interactions on the TiO<sub>2</sub> surface [41].

It is conceivable that the solubility, aggregation and electronic conjugation are dependent on the nature and position of the substituents. The molecular structures of **SD2–SD4** are well suited for

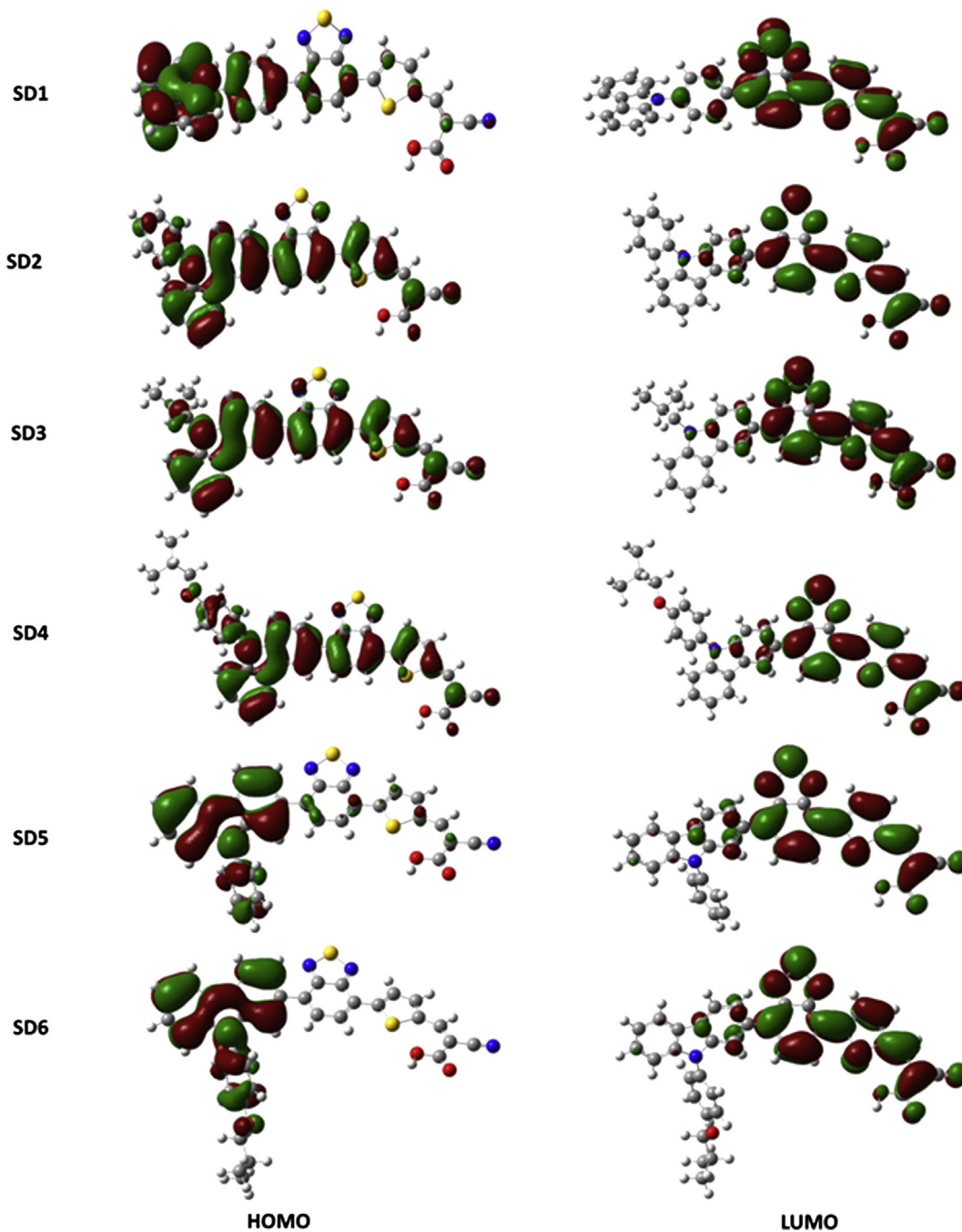


**Fig. 4.** The optimized geometric structure of synthesized dyes and their frontier orbitals were calculated by density functional theory at the B3LYP/6-31G(d) level.

better organization on  $\text{TiO}_2$  surface and overall performance than other molecules. It is clear that the chemical nature of substituents and position of the substituents play an important role in the performance of the DSSCs.

**Table 2**  
Theoretical calculations of synthesized dye molecules.

Dye	Dihedral angle ( $\alpha$ )	HOMO (eV)	LUMO (eV)	$E_g$ (eV)
<b>SD1</b>	36.3	−5.497	−3.265	2.231
<b>SD2</b>	37.3	−5.497	−3.048	2.449
<b>SD3</b>	36.9	−5.469	−3.020	2.449
<b>SD4</b>	36.6	−5.388	−3.020	2.367
<b>SD5</b>	37.2	−5.660	−3.102	2.558
<b>SD6</b>	37.7	−5.524	−3.075	2.449

### 3. Experimental details

#### 3.1. Materials

All chemicals and reagents were purchased from commercial suppliers (Sigma-Aldrich, and Merck) and used without further purification. Solvents used for spectroscopic measurements were spectral grade quality. Tetrahydrofuran (THF) was distilled over sodium metal. All reactions were monitored by thin-layer chromatography (TLC) carried out on silica gel plates. Preparative separations were performed by column chromatography on silica gel grade 60 (0.040–0.063 mm) from Merck. The starting materials 9-[4-(4,4,5,5-tetramethyl-1,3,2-dioxaborolan-2-yl)phenyl]-9H-carbazole [42], 9-phenyl-3-(4,4,5,5-tetramethyl-1,3,2-dioxaborolan-2-yl)-9H-

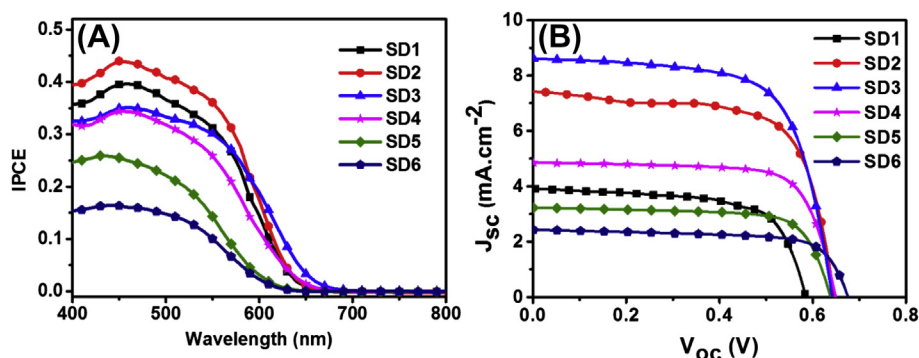


Fig. 5. Photocurrent action spectra of the DSSCs based on dyes **SD1–SD6**. (A) IPCE curves and (B)  $J$ – $V$  curves.

carbazole [43], 9-phenyl-2-(4,4,5,5-tetramethyl-1,3,2-dioxaborolan-2-yl)-9H-carbazole [44] were prepared by adopting literature procedures.

### 3.2. Analytical instruments

$^1\text{H}$  and  $^{13}\text{C}$  NMR spectra were recorded on a Bruker 300 MHz and 75 MHz spectrometer. IR spectra were measured on a Varian Bio-Rad Excalibur FT-IR spectroscopy spectrum as KBr disc. EI-mass spectra were obtained on a Finnigan MAT 95XL-T mass spectrometer. The UV–vis spectra were measured on a Shimadzu UV-1601 PC spectrophotometer. Thermogravimetric analysis (TGA) and differential scanning calorimetry analysis was performed under nitrogen atmosphere on TA Instruments Q100 at a heating rate of  $10\text{ }^\circ\text{C}/\text{min}$ . Photoluminescence spectra were recorded with a Shimadzu RF-5301 PC spectrofluorophotometer as a dilute solution in THF. Elemental analysis was carried out on Elementar Vario Micro Cube instrument.

Cyclic voltammetry was recorded with a computer controlled CHI electrochemical analyzer at a constant scan rate of  $100\text{ mV}/\text{s}$ . Measurements were performed in an electrolyte solution of  $0.1\text{ M}$  tetrabutylammoniumhexafluorophosphate dissolved in a degassed dichloromethane. The electrochemical cell consists of platinum disc as working electrode, platinum rod as counter electrode and standard calomel electrode as a reference electrode. The potentials are calibrated using ferrocene as internal standard. The onset of oxidation ( $E_{\text{ox}}^{\text{onset}}$ ) and reduction ( $E_{\text{red}}^{\text{onset}}$ ) were used to calculate HOMO and LUMO energy level using the relationship  $E_{\text{HOMO}} = -(4.8 + E_{\text{ox}}^{\text{onset}})$  and  $E_{\text{LUMO}} = -(4.8 + E_{\text{red}}^{\text{onset}})$ , respectively [44]. Geometry optimizations were performed in Gaussian 09 [45] at the density functional theory (DFT) level with the B3LYP function and a 6-31G\* basis set. The HOMO and LUMO surfaces were generated from the optimized geometries using GaussView 5 [46].

Dye sensitized solar cells (DSSCs) were fabricated using molecules **SD1–SD6** and  $\text{TiO}_2$  electrodes with a double layer structure consisting of  $12\text{ }\mu\text{m}$  thickness transparent layer with  $20\text{ nm}$  sized  $\text{TiO}_2$  nanoparticles and  $4\text{ }\mu\text{m}$  thickness scattering layer with  $400\text{ nm}$  sized  $\text{TiO}_2$  nanoparticles. The electrodes were immersed

into a  $0.25\text{ mM}$  solution of sensitizer in tetrahydrofuran and left overnight before being removed and rinsed in tetrahydrofuran immediately before cell assembly. Photoanodes and platinized counter electrodes were sealed together in a sandwich configuration and were filled with an electrolyte ( $0.6\text{ M}$  propyl methyl imidazolium iodide,  $0.03\text{ M}$   $\text{I}_2$ ,  $0.1\text{ M}$  guanidine thiocyanate and  $0.5\text{ M}$  tributyl phosphate in the solution of 85:15 ratio of acetonitrile and valeronitrile) by vacuum back-filling.

### 3.3. Synthesis of starting material for SD4 and SD6 compounds

#### 3.3.1. 9-(4-(2-Ethylhexyl)oxyphenyl)-9H-carbazole (9)

A mixture of carbazole ( $5\text{ g}$ ,  $30\text{ mmol}$ ), 4-[(2-ethylhexyl)oxy]iodobenzene ( $13\text{ g}$ ,  $39\text{ mmol}$ ),  $\text{K}_2\text{CO}_3$  ( $12.47\text{ g}$ ,  $90\text{ mmol}$ ) in DMSO ( $150\text{ mL}$ ) was stirred and refluxed under  $\text{N}_2$  for  $30\text{ min}$ . Followed by addition of  $\text{CuI}$  ( $1\text{ g}$ ,  $10\text{ mol}\%$ ) and L-proline ( $1.48\text{ g}$ ,  $12.9\text{ mmol}$ ). This mixture is refluxed at  $100\text{ }^\circ\text{C}$  under nitrogen for  $24\text{ h}$ . The reaction mixture was poured into water and extracted using diethyl ether. The crude product was purified by column chromatography using hexane as eluent to give white compound ( $6.70\text{ g}$ ,  $60\%$  yield). MS (EI)  $m/z$ :  $371.3\text{ (M}^+)$ ,  $371.22\text{ (calcd.)}$ .  $^1\text{H NMR}$  ( $300\text{ MHz}$ ,  $\text{CDCl}_3$   $\delta$  ppm):  $8.15\text{ (d, } J = 7.7\text{ Hz, 2H)}$ ,  $7.45\text{--}7.28\text{ (m, 8H)}$ ,  $7.11\text{ (d, } J = 8.8, 2\text{H, N-phenyl)}$ ,  $3.95\text{ (d, } J = 5.5\text{ Hz, 2H, } -\text{O}-\text{CH}_2-)$ ,  $1.85\text{--}1.77\text{ (m, 1H, } -\text{CH-)}$ ,  $1.53\text{--}1.37\text{ (m, 8H, } -\text{CH}_2-)$ ,  $1.02\text{--}0.93\text{ (m, 6H, } -\text{CH}_3)$ .  $^{13}\text{C NMR}$  ( $75\text{ MHz}$ ,  $\text{CDCl}_3$   $\delta$  ppm):  $158.6, 141.3, 129.9, 128.4, 125.7, 123, 120.2, 119.5, 115.5, 109.7, 70.8, 39.4, 30.5, 29.1, 23.8, 23.0, 14.1, 11.1$ . Elem. Anal. Calcd. for  $\text{C}_{26}\text{H}_{29}\text{NO}$ : C,  $84.06\%$ ; H,  $7.87\%$ ; N,  $3.77\%$ ; found: C,  $84.14\%$ ; H,  $7.68\%$ ; N,  $3.79\%$ .

#### 3.3.2. 9-(4-(2-Ethylhexyl)oxyphenyl)-3-bromo-9H-carbazole (10)

Solution of compound **9** ( $4.41\text{ g}$ ,  $11.8\text{ mmol}$ ) in  $30\text{ mL}$  DMF was stirred for  $20\text{ min}$  under nitrogen atmosphere in an ice bath. N-Bromosuccinimide ( $2.10\text{ g}$ ,  $11.8\text{ mmol}$ ) was added to it in a small portion. The reaction was allowed to run overnight. The product was extracted using dichloromethane. The organic layer was collected, dried over anhydrous  $\text{Na}_2\text{SO}_4$  and concentrated to complete dryness. The crude product was purified by column chromatography using hexane as eluent to give a colourless liquid ( $4.34\text{ g}$ ,  $56\%$  yield). MS (EI)  $m/z$ :  $451.2\text{ (M}^+)$ ,  $451.13\text{ (calcd.)}$ .  $^1\text{H NMR}$  ( $300\text{ MHz}$ ,  $\text{CDCl}_3$   $\delta$  ppm):  $8.23\text{ (s, 1H, } -\text{CAR)}$ ,  $8.08\text{ (d, } J = 7.8\text{ Hz, 1H, } -\text{CAR)}$ ,  $7.48\text{--}7.37\text{ (m, 3H, } -\text{CAR)}$ ,  $7.32\text{--}7.27\text{ (m, 2H, N-phenyl)}$ ,  $7.19\text{ (d, } J = 8.7\text{ Hz, 1H, } -\text{CAR)}$ ,  $7.10\text{ (d, } J = 8.8, 2\text{H, N-phenyl)}$ ,  $3.94\text{ (d, } J = 5.76\text{ Hz, 2H, } -\text{O}-\text{CH}_2-)$ ,  $1.81\text{--}1.75\text{ (m, 1H, } -\text{CH-)}$ ,  $1.52\text{--}1.35\text{ (m, 8H, } -\text{CH}_2-)$ ,  $1.00\text{--}0.88\text{ (m, 6H, } -\text{CH}_3)$ ;  $^{13}\text{C NMR}$  ( $75\text{ MHz}$ ,  $\text{CDCl}_3$   $\delta$  ppm):  $158.9, 141.7, 140.0, 129.4, 128.5, 128.4, 126.5, 124.7, 122.9, 122.0, 120.3, 119.9, 119.5, 115.6, 111.2, 109.9, 70.8, 39.4, 30.5, 29.1, 23.8, 23.0, 14.0, 11.1$ . Elem. Anal. Calcd. for  $\text{C}_{26}\text{H}_{28}\text{BrNO}$ : C,  $69.33\%$ ; H,  $6.27\%$ ; Br,  $17.74\%$ ; N,  $3.11\%$ ; found: C,  $69.39\%$ ; H,  $6.22\%$ ; Br,  $17.83\%$ ; N,  $3.16\%$ .

Table 3  
Performances parameters of DSSCs of carbazole dyes.

Compd.	$J_{\text{sc}}$ ( $\text{mA}/\text{cm}^2$ )	$V_{\text{oc}}$ (V)	Fill factor (%)	$\eta$ (%)
<b>SD1</b>	3.90	0.59	68.1	1.56
<b>SD2</b>	7.37	0.65	68.6	3.29
<b>SD3</b>	8.30	0.64	73.8	3.80
<b>SD4</b>	4.85	0.65	73.5	2.36
<b>SD5</b>	3.22	0.64	73.0	1.53
<b>SD6</b>	2.43	0.67	71.1	1.20

### 3.3.3. 9-(4-(2-Ethylhexyl)oxyphenyl)-3-(4,4,5,5-tetramethyl-1,3,2-dioxaborolan-2-yl)-9H-carbazole (**4**)

N-Butyl lithium (10 mL, 19.26 mmol) was added drop wise to compound **7** in dried THF solution at  $-78^{\circ}\text{C}$  and the stirred for 20 min. 2-isopropoxy-4,4,5,5-tetramethyl-[1,3,2] dioxaborolane (3.58 g, 19.26 mmol) was added slowly at  $-78^{\circ}\text{C}$  stirred for 2 h under this condition and then stirred overnight under room temperature. The solvent was evaporated and the residue was dissolved in hexane, dichloromethane mixture (2:1) and filtered. The crude product was purified by column chromatography using 5% ethyl acetate in hexane to give a colourless liquid (3.02 g, 63% yield). MS (EI)  $m/z$ : 497.3 ( $\text{M}^+$ ), 497.31 (calcd.).  $^1\text{H}$  NMR ( $\delta$ , 300 MHz,  $\text{CDCl}_3$ ) ppm: 8.64 (s, 1H,  $-\text{CAR}$ ), 8.17 (d,  $J = 7.56$ , 1H,  $-\text{CAR}$ ), 7.85 (d,  $J = 8.2$  Hz, 1H,  $-\text{CAR}$ ), 7.43–7.37 (m, 3H), 7.33–7.28 (m, 3H), 7.10 (d,  $J = 8.8$  Hz, 2H, N-phenyl), 3.94 (d,  $J = 5.7$ , 2H,  $-\text{O}-\text{CH}_2-$ ), 1.85–1.75 (m, 1H,  $-\text{CH}-$ ), 1.54–1.40 (m, 20H), 1.00–0.88 (m, 6H,  $-\text{CH}_3$ ).  $^{13}\text{C}$  NMR (75 MHz,  $\text{CDCl}_3$   $\delta$  ppm): 158.7, 143.4, 141.5, 132.2, 129.7, 128.4, 127.6, 125.7, 123.2, 122.8, 120.4, 119.9, 119.0, 115.5, 109.7, 109.0, 83.6, 70.8, 39.4, 30.5, 29.1, 24.9, 23.8, 23.0, 14.0, 11.1. Elem. Anal. Calcd. for  $\text{C}_{32}\text{H}_{40}\text{BNO}_3$ : C, 77.26%; H, 8.10%; N, 2.82%; found: C, 77.20%; H, 8.19%; N, 2.75%.

### 3.3.4. 9-(4-(2-Ethylhexyl)oxyphenyl)-2-bromo-9H-carbazole (**12**)

A mixture of 9-phenyl-2-bromo-9H-carbazole (1.95 g, 8 mmol), 4-[(2-ethylhexyloxy)-iodobenzene (3.5 g, 10.4 mmol),  $\text{K}_2\text{CO}_3$  (12.47 g, 90 mmol) in DMSO (150 mL) was stirred and refluxed under  $\text{N}_2$  for 30 min, followed by addition of CuI (1 g, 10 mol%) and L-proline (1.48 g, 3.44 mmol). This mixture was refluxed at  $100^{\circ}\text{C}$  under nitrogen atmosphere for 24 h. The reaction mixture was poured into water and extracted using diethyl ether. The crude product was purified by column chromatography using hexane as eluent to give white product (1.79 g, 50% yield). MS (EI)  $m/z$ : 451.2 ( $\text{M}^+$ ), 451.13 (calcd.).  $^1\text{H}$  NMR (300 MHz,  $\text{CDCl}_3$   $\delta$  ppm): 8.09 (d,  $J = 7.89$  Hz, 1H,  $-\text{CAR}$ ), 7.97 (d,  $J = 8.22$  Hz, 1H,  $-\text{CAR}$ ), 7.64 (s, 1H,  $-\text{CAR}$ ), 7.56–7.28 (m, 6H), 7.11 (d,  $J = 8.7$  Hz, 2H, N-phenyl), 3.95 (d,  $J = 5.5$ , 2H,  $-\text{O}-\text{CH}_2-$ ), 1.82–1.78 (m, 1H,  $-\text{CH}-$ ), 1.52–1.36 (m, 8H), 1.01–0.94 (m, 6H,  $-\text{CH}_3$ ).  $^{13}\text{C}$  NMR (75 MHz,  $\text{CDCl}_3$   $\delta$  ppm): 158.9, 141.7, 140.0, 129.4, 128.5, 128.4, 126.5, 124.7, 122.9, 122.0, 120.3, 119.9, 119.5, 115.6, 111.2, 109.9, 70.8, 39.4, 30.5, 29.1, 23.8, 23.0, 14.0, 11.1. Elem. Anal. Calcd. for  $\text{C}_{26}\text{H}_{28}\text{BrNO}$ : C, 69.33%; H, 6.27%; Br, 17.74%; N, 3.11%; found: C, 69.35%; H, 6.32%; Br, 17.80%; N, 3.14%.

### 3.3.5. 9-(4-(2-Ethylhexyl)oxyphenyl)-2-(4,4,5,5-tetramethyl-1,3,2-dioxaborolan-2-yl)-9H-carbazole (**6**)

N-Butyl lithium (4 mL, 8 mmol) was added drop wise to compound **8** (1.8 g, 4 mmol) in dried THF solution at  $-78^{\circ}\text{C}$  and the stirred for 20 min. 2-Isopropoxy-4,4,5,5-tetramethyl-[1,3,2] dioxaborolane (1.488 g, 8 mmol) was added slowly at  $-78^{\circ}\text{C}$  stirred for 2 h and left stirring at room temperature for 6 h. The solvent was evaporated, the residue dissolved in hexane–DCM mixture (2:1) and filtered. The crude product was purified by column chromatography using 5% ethyl acetate in hexane to give a white solid (600 mg, 30% yield). MS (EI)  $m/z$ : 497.4 ( $\text{M}^+$ ), 497.31 (calcd.).  $^1\text{H}$  NMR (300 MHz,  $\text{CDCl}_3$   $\delta$  ppm): 8.16–8.12 (m, 2H,  $-\text{CAR}$ ), 7.77 (s, 1H,  $-\text{CAR}$ ), 7.73 (d,  $J = 7.8$  Hz, 1H,  $-\text{CAR}$ ), 7.44–7.38 (m, 3H,  $-\text{CAR}$ ), 7.30 (d,  $J = 8.4$  Hz, 2H, N-phenyl), 7.11 (d,  $J = 8.8$  Hz, 2H, N-phenyl), 3.96 (d,  $J = 5.6$ , 2H,  $-\text{O}-\text{CH}_2-$ ), 1.84–1.76 (m, 1H,  $-\text{CH}-$ ), 1.50–1.37 (m, 20H), 1.01–0.85 (m, 6H,  $-\text{CH}_3$ ).  $^{13}\text{C}$  NMR (75 MHz,  $\text{CDCl}_3$   $\delta$  ppm): 158.7, 142.0, 140.9, 129.9, 128.7, 126.3, 125.8, 125.5, 122.7, 122.2, 120.6, 119.5, 119.4, 116.0, 115.6, 109.8, 83.7, 70.8, 39.4, 30.5, 29.1, 24.8, 23.9, 23.0, 14.1, 11.1. Elem. Anal. Calcd. for  $\text{C}_{32}\text{H}_{40}\text{BNO}_3$ : C, 77.26%; H, 8.10%; N, 2.82%; found: C, 77.24%; H, 8.14%; N, 2.79%.

### 3.4. General synthesis of the precursors **1a**, **2a**, **3a**, **4a**, **5a** and **6a**

Compounds **1a**, **2a**, **3a**, **4a**, **5a** were synthesized from 4,7-dibromobenzo[1,2,5]thiadiazole reaction with N-phenyl carbazole boronic ester using Suzuki coupling reaction. Method described for **1a** was used for rest of the compounds. A stirred mixture of 4,7-dibromobenzo[1,2,5]thiadiazole (0.293 g, 1 mmol), **1** (0.368 g, 1 mmol),  $\text{Pd}(\text{PPh}_3)_4$  (60 mg, 0.05 mmol),  $\text{K}_2\text{CO}_3$  (2 M, 5 mL) in THF (20 mL) was heated at  $70$ – $80^{\circ}\text{C}$  under  $\text{N}_2$  atmosphere for 24 h. When the reaction was complete, water was added to quench the reaction. The product was extracted with dichloromethane. The organic layer was collected, dried over anhydrous  $\text{Na}_2\text{SO}_4$  and concentrated to dryness. The solid was adsorbed on silica and purified by column chromatography using a mixture of dichloromethane–hexane (1:4) as eluent to give **1a**, yellow solid (186 mg, 40% yield).

#### 3.4.1. 4-(4-(9H-carbazol-9-yl)phenyl)-7-bromobenzo[1,2,5]thiadiazole (**1a**)

Yellow solid (0.186 g, 40.7% yield), MS (EI)  $m/z$ : 457.1 ( $\text{M}^+$ ), 455.01 (calcd.).  $^1\text{H}$  NMR (300 MHz,  $\text{CDCl}_3$   $\delta$  ppm): 8.16 (d,  $J = 8.55$  Hz, 4H,  $-\text{phenyl}$ ), 7.99 (d,  $J = 7.56$  Hz, 1H,  $-\text{BTZ}$ ), 7.76 (d,  $J = 8.55$  Hz, 2H,  $-\text{CAR}$ ), 7.70 (d,  $J = 7.56$  Hz, 1H,  $-\text{BTZ}$ ), 7.54 (d,  $J = 8.22$  Hz, 2H,  $-\text{CAR}$ ), 7.44 (t, 2H,  $-\text{CAR}$ ), 7.31 (t, 2H,  $-\text{CAR}$ ).  $^{13}\text{C}$  NMR (75 MHz,  $\text{CDCl}_3$   $\delta$  ppm): 153.9, 153.0, 140.6, 138.1, 135.4, 132.9, 132.3, 130.6, 128.4, 127.1, 126.0, 123.5, 120.3, 120.1, 113.6, 109.8. Elem. Anal. Calcd. for  $\text{C}_{24}\text{H}_{14}\text{BrN}_3\text{S}$ : C, 63.16%; H, 3.09%; N, 9.21%; S, 7.03%; Br, 17.51%; found: C, 63.21%; H, 3.20%; N, 9.39%; S, 7.10%; Br, 17.37%.

#### 3.4.2. 4-Bromo-7-(9-phenyl-9H-carbazol-3-yl)benzo[1,2,5]thiadiazole (**2a**)

Yellow solid (0.215 g, 47% yield), MS (EI)  $m/z$ : 457.1 ( $\text{M}^+$ ), 455.01 (calcd.).  $^1\text{H}$  NMR (300 MHz,  $\text{CDCl}_3$   $\delta$  ppm): 8.67 (s, 1H,  $-\text{CAR}$ ), 8.22 (d,  $J = 7.74$  Hz, 1H,  $-\text{BTZ}$ ), 7.96 (d,  $J = 8.4$  Hz, 2H), 7.68 (m, 1H,  $-\text{BTZ}$ ), 7.61 (m, 4H), 7.53 (m, 2H), 7.44 (d,  $J = 3.3$  Hz, 2H,  $-\text{CAR}$ ), 7.35–7.30 (m, 1H, N-phenyl).  $^{13}\text{C}$  NMR (75 MHz,  $\text{CDCl}_3$   $\delta$  ppm): 153.8, 143.3, 140.9, 137.3, 134.8, 132.3, 129.9, 129.1, 128.4, 127.8, 127.6, 127.1, 127.0, 126.2, 123.7, 123.3, 121.1, 120.4, 120.2, 112.0, 109.96, 109.90. Elem. Anal. Calcd. for  $\text{C}_{24}\text{H}_{14}\text{BrN}_3\text{S}$ : C, 63.16%; H, 3.09%; N, 9.21%; S, 7.03%; Br, 17.51%; found: C, 63.27%; H, 3.18%; N, 9.38%; S, 7.18%; Br, 17.62%.

#### 3.4.3. 3-(7-bromo-benzo[1,2,5]thiadiazol-4-yl)-9-(2-ethyl-hexyl)-9H-carbazole (**3a**)

Yield of an orange oil, (0.148 g) 30%. MS (EI)  $m/z$ : 493.1 ( $\text{M}^+$ ), 493.10 (Calcd.).  $^1\text{H}$  NMR (300 MHz,  $\text{CDCl}_3$   $\delta$  ppm): 8.63 (s, 1H,  $-\text{CAR}$ ), 8.17 (d,  $J = 7.7$  Hz, 1H,  $-\text{BTZ}$ ), 8.01–8.04 (dd, 1H,  $-\text{BTZ}$ ), 7.94 (d,  $J = 7.6$  Hz,  $-\text{CAR}$ ), 7.67 (d,  $J = 7.7$  Hz,  $-\text{CAR}$ ), 7.42–7.54 (m, 3H,  $-\text{CAR}$ ), 7.24–7.29 (t, 1H,  $-\text{CAR}$ ), 4.15–4.28 (m, 2H,  $-\text{CH}_2$ ), 2.10 (t, 1H,  $-\text{CH}-$ ), 1.25–1.42 (m, 8H,  $-\text{CH}_2$ ), 0.86–0.96 (m, 6H,  $-\text{CH}_3$ ).  $^{13}\text{C}$  NMR (75 MHz,  $\text{CDCl}_3$   $\delta$  ppm): 154.0, 153.6, 141.4, 141.1, 135.0, 132.4, 127.8, 127.3, 126.9, 126.0, 123.2, 122.9, 121.2, 120.5, 119.1, 111.8, 109.2, 109.1, 47.6, 39.5, 31.0, 28.8, 24.4, 23.1, 14.1, 10.9. Elem. Anal. Calcd. for  $\text{C}_{26}\text{H}_{26}\text{BrN}_3\text{S}$ : C, 63.41%; H, 5.32%; N, 8.53%; S, 6.51%; Br, 16.23%; found: C, 63.47%; H, 5.26%; N, 8.53%; S, 6.55%; Br, 16.26%.

#### 3.4.4. 4-Bromo-7-(9-(4-(2-ethylhexyloxy)phenyl)-9H-carbazol-3-yl)benzo[1,2,5]thiadiazole (**4a**)

Yellow solid (0.182 g, 36% yield), MS (EI)  $m/z$ : 585.2 ( $\text{M}^+$ ), 585.13 (calcd.).  $^1\text{H}$  NMR (300 MHz,  $\text{CDCl}_3$   $\delta$  ppm): 8.66 (s, 1H,  $-\text{CAR}$ ), 8.20 (d,  $J = 7.6$  Hz, 1H), 7.95 (d,  $J = 7.8$  Hz, 2H), 7.67 (d,  $J = 7.5$  Hz, 1H), 7.48–7.28 (m, 6H), 7.13 (d,  $J = 8.8$  Hz, 2H), 3.96 (d,  $J = 5.76$  Hz, 2H,  $-\text{O}-\text{CH}_2-$ ), 1.85–1.75 (m, 1H,  $-\text{CH}-$ ), 1.53–1.35 (m, 8H), 1.00–0.92 (t, 6H,  $-\text{CH}_3$ ).  $^{13}\text{C}$  NMR (75 MHz,  $\text{CDCl}_3$   $\delta$  ppm): 158.8, 153.9, 153.5, 141.9, 141.5, 134.9, 132.4, 129.6, 128.4, 128.2, 127.8, 127.1, 126.2, 123.4, 123.1, 121.2, 120.4, 119.9, 115.6, 111.9, 109.98, 198.91, 70.8, 39.3, 30.5, 29.1, 23.8, 23.0, 14.1, 11.1. Elem. Anal. Calcd. for

C<sub>32</sub>H<sub>30</sub>BrN<sub>3</sub>OS: C, 65.75%; H, 5.17%; N, 7.19%; S, 5.49%; Br, 13.67%; found: C, 65.89%; H, 5.38%; N, 7.24%; S, 5.52%; Br, 13.83%.

#### 3.4.5. 4-Bromo-7-(9-phenyl-9H-carbazol-2-yl)benzo[1,2,5]thiadiazole (**5a**)

Yellow solid (0.150 g, 32% yield), MS (EI) *m/z*: 457.0 (M<sup>+</sup>), 457.01 (calcd.). <sup>1</sup>H NMR (300 MHz, CDCl<sub>3</sub> δ ppm): 8.27 (d, *J* = 8.1 Hz, 1H), 8.19 (d, *J* = 7.74 Hz, 1H), 7.97–7.88 (m, 2H), 7.81 (d, *J* = 8.0 Hz, 1H), 7.63–7.58 (m, 5H), 7.45–7.43 (m, 3H), 7.35–7.30 (m, 1H, N-phenyl). <sup>13</sup>C NMR (75 MHz, CDCl<sub>3</sub> δ ppm): 153.8, 153.3, 141.6, 141.0, 137.4, 134.8, 134.3, 132.2, 129.9, 128.4, 127.5, 127.1, 126.4, 123.6, 122.9, 121.2, 120.5, 120.4, 120.2, 112.7, 110.6, 109.9. Elem. Anal. Calcd. for C<sub>24</sub>H<sub>14</sub>BrN<sub>3</sub>S: C, 63.16%; H, 3.09%; N, 9.21%; S, 7.03%; Br, 17.51%; found: C, 63.21%; H, 3.26%; N, 9.39%; S, 7.24%; Br, 17.44%.

#### 3.4.6. 4-Bromo-7-(9-(4-(2-ethylhexyloxy)phenyl)-9H-carbazol-2-yl)benzo[1,2,5]thiadiazole (**6a**)

Yellow solid (0.08 g, 30% yield), MS (EI) *m/z*: 585.2 (M<sup>+</sup>), 585.13 (calcd.). <sup>1</sup>H NMR (300 MHz, CDCl<sub>3</sub> δ ppm): 8.26 (d, *J* = 8.5 Hz, 1H), 8.18 (d, *J* = 7.7 Hz, 1H), 7.90 (d, *J* = 7.5 Hz, 1H), 7.82 (m, 2H), 7.60 (d, *J* = 7.7 Hz, 1H), 7.48 (d, *J* = 8.8 Hz, 2H), 7.44–7.28 (m, 3H), 7.12 (d, *J* = 9 Hz, 2H, N-phenyl), 3.93 (d, *J* = 5.7, 2H, –O–CH<sub>2</sub>–), 1.83–1.72 (m, 1H, –CH–), 1.54–1.39 (m, 8H, –CH<sub>2</sub>–), 0.99–0.90 (m, 6H, –CH<sub>3</sub>–). <sup>13</sup>C NMR (75 MHz, CDCl<sub>3</sub> δ ppm): 158.8, 153.8, 153.4, 142.1, 141.5, 134.9, 134.2, 132.2, 129.7, 128.5, 128.4, 126.3, 123.4, 122.7, 121.0, 120.5, 120.3, 119.9, 115.6, 112.6, 110.5, 109.89, 70.88, 39.4, 30.5, 29.1, 23.8, 23.0, 14.0, 11.1. Elem. Anal. Calcd. for C<sub>32</sub>H<sub>30</sub>BrN<sub>3</sub>OS: C, 65.75%; H, 5.17%; N, 7.19%; S, 5.49%; Br, 13.67%; found: C, 65.66%; H, 5.32%; N, 7.15%; S, 5.62%; Br, 13.84%.

### 3.5. Synthesis of the aldehydes **1b**, **2b**, **3b**, **4b**, **5b** and **6b**

Compounds **1b**, **2b**, **3b**, **4b**, **5b** and **6b** were synthesized from 5-formylthienyl-2-boronic acid with corresponding bromides (**1a**, **2a**, **3a**, **4a**, **5a** and **6a**) using Suzuki coupling reaction. Only preparation of **1c** will be discussed in detail.

A stirred mixture of **1a** (0.16 g, 0.35 mmol), 5-formylthienyl-2-boronic acid (0.16 g, 1.05 mmol), Pd(PPh<sub>3</sub>)<sub>4</sub> (0.025 g, 0.05 mmol), K<sub>2</sub>CO<sub>3</sub> (2 M aqueous solution, 4 mL) in THF (20 mL) was heated at 70–80 °C under N<sub>2</sub> atmosphere for 24 h. When the reaction was complete, water was added to quench the reaction. The product was extracted with dichloromethane and organic layers were collected, dried over anhydrous Na<sub>2</sub>SO<sub>4</sub> and concentrated to complete dryness. The solid was adsorbed on silica and purified by column chromatography, using 5% ethyl acetate/hexane mixture as eluent to give orange colour solid (0.092 g, 54% yield).

#### 3.5.1. 5-(7-(4-(9H-carbazol-9-yl)phenyl)benzo[1,2,5]thiadiazol-4-yl)thiophene-2-carbaldehyde (**1b**)

Dark orange solid (0.092 g, 54% yield), MS (EI) *m/z*: 487.2 (M<sup>+</sup>), 487.08 (calcd.). <sup>1</sup>H NMR (300 MHz, CDCl<sub>3</sub> δ ppm): 10.0 (s, 1H, –CHO), 8.28–8.23 (m, 3H), 8.18–8.13 (m, 3H), 7.91 (d, *J* = 7.5 Hz, 2H), 7.78 (d, *J* = 8.5 Hz, 2H), 7.56 (d, *J* = 8.37 Hz, 2H), 7.45 (t, 2H, –CAR), 7.32 (t, 2H, –CAR). <sup>13</sup>C NMR (75 MHz, CDCl<sub>3</sub> δ ppm): 183.2, 148.5, 143.5, 140.6, 138.2, 136.9, 136.7, 135.6, 133.9, 130.7, 128.2, 127.9, 127.4, 127.0, 126.5, 126.0, 125.3, 123.5, 120.3, 120.2, and 109.8. Elem. Anal. Calcd. for C<sub>29</sub>H<sub>17</sub>N<sub>3</sub>O<sub>2</sub>S: C, 71.43%; H, 3.51%; N, 8.62%; S, 13.15%; found: C, 71.34%; H, 3.83%; N, 8.54%; S, 13.37%.

#### 3.5.2. 5-(7-(9-Phenyl-9H-carbazol-3-yl)benzo[1,2,5]thiadiazol-4-yl)thiophene-2-carbaldehyde (**2b**)

Brick red solid (0.05 g, 30% yield), MS (EI) *m/z*: 487.1 (M<sup>+</sup>), 487.08 (calcd.). <sup>1</sup>H NMR (300 MHz, CDCl<sub>3</sub> δ ppm): 9.99 (s, 1H, –CHO), 8.76 (s, 1H, –CAR), 8.24 (m, 2H), 8.10 (d, *J* = 7.56 Hz, 1H), 8.04 (d, *J* = 7.5, 1H, –BTZ), 7.88 (d, *J* = 6.0 Hz, 2H), 7.64–7.51 (m, 6H), 7.44 (d, *J* = 2.2,

2H), 7.36–7.31 (m, 1H, N-phenyl). <sup>13</sup>C NMR (75 MHz, CDCl<sub>3</sub> δ ppm): 183.0, 154.2, 152.7, 149.0, 143.2, 141.4, 141.1, 137.3, 136.8, 135.9, 129.9, 128.7, 127.8, 127.75, 127.70, 127.37, 127.34, 127.1, 126.3, 124.0, 123.7, 123.4, 121.4, 120.5, 120.3, 110.0, 109.9. Elem. Anal. Calcd. for C<sub>29</sub>H<sub>17</sub>N<sub>3</sub>O<sub>2</sub>S: C, 71.43%; H, 3.51%; N, 8.62%; S, 13.15%; found: C, 71.35%; H, 3.66%; N, 8.48%; S, 13.27%.

#### 3.5.3. 5-(7-(9-(2-ethyl-hexyl)-9H-carbazol-3-yl)-benzo[1,2,5]thiadiazol-4-yl)thiophene-2-carbaldehyde (**3b**)

Yield is (0.450 g) 86%. MS (EI) *m/z*: 523.2 (M<sup>+</sup>), 523.18 (Calcd.). <sup>1</sup>H NMR (300 MHz, CDCl<sub>3</sub> δ ppm): 10.00 (s, 1H, –CHO), 8.73 (b, 1H, –CAR), 8.25 (d, *J* = 4.1 Hz, 1H, –BTZ), 8.19 (d, *J* = 7.7 Hz, 1H, –CAR), 8.12 (d, *J* = 7.6 Hz, 2H), 7.88 (t, 2H), 7.43–7.57 (m, 3H, –CAR), 7.30 (d, 1H, –CAR), 4.22–4.25 (m, 2H, –CH<sub>2</sub>–), 2.13 (t, 1H, –CH–), 1.28–1.43 (m, 8H, –CH<sub>2</sub>–), 0.86–0.97 (m, 6H, –CH<sub>3</sub>). <sup>13</sup>C NMR (75 MHz, CDCl<sub>3</sub> δ ppm): δ = 182.9, 154.2, 152.7, 149.1, 143.1, 141.4, 141.2, 136.7, 136.1, 134.5, 127.7, 127.5, 127.1, 127.0, 126.0, 123.8, 123.2, 122.9, 121.3, 120.4, 119.2, 109.2, 109.1, 47.6, 39.4, 31.0, 28.8, 24.4, 23.0, 13.9, 10.8. Elem. Anal. Calcd. for C<sub>31</sub>H<sub>29</sub>N<sub>3</sub>O<sub>2</sub>S: C, 71.09%; H, 5.58%; N, 8.02%; S, 12.25%; found: C, 71.27%; H, 5.71%; N, 8.24%; S, 12.39%.

#### 3.5.4. 5-(7-(9-(4-(2-Ethylhexyloxy)phenyl)-9H-carbazol-3-yl)benzo[1,2,5]thiadiazol-4-yl)thiophene-2-carbaldehyde (**4b**)

Brick red solid (0.16 g, 80% yield), MS (EI) *m/z*: 615.4 (M<sup>+</sup>), 615.20 (calcd.). <sup>1</sup>H NMR (300 MHz, CDCl<sub>3</sub> δ ppm): 9.97 (s, 1H, –CHO), 8.73 (s, 1H, –CAR), 8.21 (d, *J* = 5.7 Hz, 2H), 8.08–7.99 (m, 2H), 7.84 (d, *J* = 3.9, 2H), 7.47–7.28 (m, 6H), 7.12 (d, *J* = 8.8, 2H), 3.96 (d, *J* = 5.5, 2H, –OCH<sub>2</sub>–), 1.83–1.77 (m, 1H, –CH–), 1.53–1.37 (m, 8H, (–CH<sub>2</sub>–)<sub>4</sub>), 1.02–0.92 (m, 6H, (–CH<sub>3</sub>)<sub>2</sub>). <sup>13</sup>C NMR (75 MHz, CDCl<sub>3</sub> δ ppm): 183.0, 158.8, 154.1, 152.6, 149.0, 143.2, 143.1, 141.9, 141.6, 136.8, 136.0, 129.5, 128.4, 127.7, 127.6, 127.3, 127.2, 126.2, 123.9, 123.5, 123.1, 121.3, 120.4, 120.0, 115.6, 110.0, 109.9, 70.85, 39.4, 30.5, 29.1, 23.8, 23.0, 14.1, 11.1. Elem. Anal. Calcd. for C<sub>37</sub>H<sub>33</sub>N<sub>3</sub>O<sub>2</sub>S<sub>2</sub>: C, 72.16%; H, 5.40%; N, 6.82%; S, 10.41%; found: C, 72.24%; H, 5.49%; N, 6.63%; S, 10.05%.

#### 3.5.5. 5-(7-(9-Phenyl-9H-carbazol-2-yl)benzo[1,2,5]thiadiazol-4-yl)thiophene-2-carbaldehyde (**5b**)

Brick red solid (0.06 mg, 40% yield), MS (EI) *m/z*: 487.1 (M<sup>+</sup>), 487.08 (calcd.). <sup>1</sup>H NMR (300 MHz, CDCl<sub>3</sub> δ ppm): 9.98 (s, 1H, –CHO), 8.29 (d, *J* = 8.07, 1H), 8.21 (m, 2H), 8.05 (d, *J* = 7.4, 1H), 8.00 (s, 1H, –CAR), 7.91–7.90 (m, 3H), 7.80 (m, 4H), 7.46–7.44 (m, 3H), 7.35–7.32 (m, 1H, N-phenyl). <sup>13</sup>C NMR (75 MHz, CDCl<sub>3</sub> δ ppm): 183.0, 154.1, 152.5, 148.8, 143.3, 141.6, 141.0, 137.4, 136.8, 135.9, 134.5, 129.9, 127.9, 127.6, 127.4, 127.1, 126.4, 125.6, 124.6, 123.8, 122.9, 121.4, 120.6, 120.4, 120.2, 110.7, 109.9. Elem. Anal. Calcd. for C<sub>29</sub>H<sub>17</sub>N<sub>3</sub>O<sub>2</sub>S: C, 71.43%; H, 3.51%; N, 8.62%; S, 13.15%; found: C, 71.26%; H, 3.57%; N, 8.61%; S, 12.93%.

#### 3.5.6. 5-(7-(9-(4-(2-Ethylhexyloxy)phenyl)-9H-carbazol-2-yl)benzo[1,2,5]thiadiazol-4-yl)thiophene-2-carbaldehyde (**6b**)

Brick red solid (0.025 g, 40% yield), MS (EI) *m/z*: 615.3 (M<sup>+</sup>), 615.20 (calcd.). <sup>1</sup>H NMR (300 MHz, CDCl<sub>3</sub> δ ppm): 9.97 (s, 1H, –CHO), 8.27 (d, *J* = 8.0 Hz, 1H), 8.21–8.17 (m, 2H), 8.04 (d, *J* = 7.4 Hz, 1H), 7.90–7.83 (m, 3H), 7.79 (d, *J* = 7.5 Hz, 1H), 7.51–7.28 (m, 5H), 7.12 (d, *J* = 8.8 Hz, 2H, N-Phenyl), 3.94 (d, *J* = 5.76 Hz, 2H, –O–CH<sub>2</sub>–), 1.83–1.75 (m, 1H, –CH–), 1.59–1.34 (m, 8H, (–CH<sub>2</sub>–)<sub>4</sub>), 0.97–0.90 (m, 6H, (–CH<sub>3</sub>)<sub>2</sub>). <sup>13</sup>C NMR (75 MHz, CDCl<sub>3</sub> δ ppm): 183.0, 158.8, 154.1, 152.5, 148.8, 143.3, 142.2, 141.5, 136.7, 136.0, 134.4, 133.8, 129.7, 128.5, 127.9, 127.4, 126.3, 124.5, 123.5, 122.7, 121.1, 120.5, 120.3, 119.9, 115.6, 110.7, 109.9, 70.8, 39.4, 30.5, 29.1, 23.8, 23.0, 14.0, 11.1. Elem. Anal. Calcd. for C<sub>37</sub>H<sub>33</sub>N<sub>3</sub>O<sub>2</sub>S<sub>2</sub>: C, 72.16%; H, 5.40%; N, 6.82%; S, 10.41%; found: C, 72.32%; H, 5.21%; N, 7.01%; S, 10.22%.

### 3.6. General synthetic procedure of dyes SD1–SD6

Compounds **SD1**, **SD2**, **SD3**, **SD4**, **SD5** and **SD6** were synthesized using similar procedures and only the synthesis of SD1 is described in detail.

To a stirred solution of compound **1b** (0.05 g, 0.102 mmol) and cyanoacetic acid (0.036 g, 0.360 mmol) in chloroform (8 mL) was added piperidine (0.059 g, 0.1 mL, 0.7 mmol). This was refluxed under N<sub>2</sub> atmosphere, cooled and acidified with 2 M HCl aqueous solution (4 mL). The crude product was extracted with CHCl<sub>3</sub>. The organic layer was collected, dried over anhydrous Na<sub>2</sub>SO<sub>4</sub> and concentrated to dryness. The product was purified using column chromatography with methanol–tetrahydrofuran mixture (1:10) as eluent to give dark brown solid.

#### 3.6.1. 2-Cyano-3-(5-(7-(4-(9H-carbazol-9-yl) phenyl)benzo[1,2,5]thiadiazol-4-yl)thiophene-2-yl)acrylic acid (**SD1**)

Dark Brown solid (0.22 g, 37% yield), MS (ESI) *m/z*: 552.7 (M<sup>+</sup>), 554.09 (calcd.). FT-IR (KBr): 3442.8 (OH stretch), 2213.5 (CN stretch), 1627.1 (CO stretch), 1450.7 (C=C aromatic stretch) and 1225.6 cm<sup>-1</sup> (C–O single bond stretch). <sup>1</sup>H NMR (300 MHz, DMSO-*d*<sub>6</sub> δ ppm): 8.36–8.32 (m, 3H), 8.27 (d, *J* = 6.5 Hz, 3H), 8.10 (d, *J* = 7.6 Hz, 2H), 7.91 (d, *J* = 4.7 Hz, 1H), 7.82 (d, *J* = 8.0 Hz, 2H), 7.53–7.44 (m, 4H), 7.31 (t, 2H). Elem. Anal. Calcd. for C<sub>32</sub>H<sub>18</sub>N<sub>4</sub>O<sub>2</sub>S<sub>2</sub>: C, 69.30%; H, 3.27%; N, 10.10%; S, 11.56%. Found: C, 69.66%; H, 3.51%; N, 10.23%; S, 11.93%.

#### 3.6.2. 2-Cyano-3-(5-(7-(9-phenyl-9H-carbazol-3-yl)benzo[1,2,5]thiadiazol-4-yl)thiophene-2-yl)acrylic acid (**SD2**)

Brown color solid (0.32 g, 68% yield), MS (MALDI) *m/z*: 553.8 (M<sup>+</sup>), 554.09 (calcd.). FT-IR (KBr): 3448.4 (OH stretch), 2219.1 (CN stretch), 1686.1 (CO stretch), 1626 (C=C alkene stretch), 1579 (C=C aromatic stretch) and 1234.4 cm<sup>-1</sup> (C–O single bond stretch). <sup>1</sup>H NMR (300 MHz, DMSO-*d*<sub>6</sub> δ ppm): 8.90 (s, 1H, –CAR), 8.50 (s, 1H, olefinic), 8.40–8.29 (m, 3H), 8.13–8.04 (m, 3H), 7.74–7.65 (m, 4H), 7.57 (t, 1H), 7.52–7.31 (m, 4H). Elem. Anal. Calcd. for C<sub>32</sub>H<sub>18</sub>N<sub>4</sub>O<sub>2</sub>S<sub>2</sub>: C, 69.30%; H, 3.27%; N, 10.10%; S, 11.56%. Found: C, 69.51%; H, 3.47%; N, 9.93%; S, 11.88%.

#### 3.6.3. 2-Cyano-3-(5-(7-(9-(2-ethyl-hexyl)-9H-carbazol-3-yl)-benzo[1,2,5]thiadiazol-4-yl)-thiophen-2-yl)acrylic acid (**SD3**)

Maroon solid (0.8 g, 61% yield). MS (MALDI) *m/z*: 590.2 (M<sup>+</sup>), 590.18 (Calcd.). FT-IR (KBr): 3435.5 (OH stretch), 3045.3 (=CH stretch), 2926.4 (–CH stretch), 2213.2 (CN stretch), 1624.6 (CO stretch), 1577.7 (C=C alkene stretch), 1535.0 (C=C aromatic stretch) and 1249.8 (C–O stretch). <sup>1</sup>H NMR (300 MHz, DMSO-*d*<sub>6</sub> δ ppm): 8.84 (b, 1H, –CAR), 8.28 (d, *J* = 7.6 Hz, 1H, –BTZ), 8.23–8.25 (m, 2H), 8.13–8.17 (m, 2H), 8.03 (d, *J* = 7.6 Hz, 1H, –BTZ), 7.85 (d, *J* = 4.0 Hz), 7.70 (d, *J* = 8.9 Hz, 1H, –CAR), 7.60 (d, *J* = 8.2 Hz, –CAR), 7.50 (t, 1H, –CAR), 7.24 (t, 1H, –CAR), 4.32 (d, *J* = 7.4 Hz, 2H, –CH<sub>2</sub>–), 2.05 (m, 1H, –CH–), 1.22–1.35 (m, 8H, –CH<sub>2</sub>–), 0.77–0.90 (m, 6H, –CH<sub>3</sub>). <sup>13</sup>C NMR (75 MHz, DMSO-*d*<sub>6</sub> δ ppm): 172.0, 153.4, 152.0, 143.4, 140.9, 140.5, 140.2, 138.2, 135.3, 135.2, 134.0, 127.9, 127.7, 127.5, 127.3, 127.2, 126.0, 123.6, 122.3, 122.2, 121.2, 120.5, 119.2, 119.1, 109.7, 109.5, 46.7, 30.2, 28.1, 23.7, 22.5, 21.1, 13.8, 10.7. Elem. Anal. Calcd. for C<sub>34</sub>H<sub>30</sub>N<sub>4</sub>O<sub>2</sub>S<sub>2</sub>: C, 69.13%; H, 5.12%; N, 9.48%; S, 10.86%. Found: C, 69.45%; H, 5.31%; N, 9.71%; S, 10.68%.

#### 3.6.4. 2-Cyano-3-(5-(7-(9-(4-(2-ethylhexyloxy)phenyl)-9H-carbazol-3-yl)benzo[1,2,5]thiadiazol-4-yl) thiophene-2-yl)acrylic acid (**SD4**)

Dark Brown solid (0.21 g, 40% yield), MS (MALDI) *m/z*: 682.57 (M<sup>+</sup>), 682.21 (calcd.). FT-IR (KBr): 3443.0 (OH stretch), 3045.7 (=CH stretch), 2927.1 (–CH stretch), 2216.8 (CN stretch), 1707.5 (CO stretch), 1623.1 (C=C alkene stretch), 1514.3 (C=C

aromatic stretch) and 1245.8 cm<sup>-1</sup> (C–O single bond stretch). <sup>1</sup>H NMR (300 MHz, DMSO-*d*<sub>6</sub> δ ppm): 8.9 (s, 1H, –CAR), 8.39–8.30 (m, 4H), 8.15–8.07 (m, 2H), 8.01 (d, *J* = 4.2 Hz, 1H), 7.56 (d, *J* = 8.4 Hz, 2H), 7.47 (t, 2H), 7.35 (t, 2H), 7.24 (d, 2H, N-phenyl), 3.99 (d, *J* = 5.5 Hz, 2H, –O–CH<sub>2</sub>–), 1.76 (m, 1H, –CH–), 1.50–1.35 (m, 8H, –CH<sub>2</sub>–), 0.97–0.91 (m, 6H, –CH<sub>3</sub>–). Elem. Anal. Calcd. for C<sub>40</sub>H<sub>34</sub>N<sub>4</sub>O<sub>3</sub>S<sub>2</sub>: C, 70.36%; H, 5.02%; N, 8.20%; S, 9.39%. Found: C, 70.19%; H, 5.32%; N, 8.11%; S, 9.89%.

#### 3.6.5. 2-Cyano-3-(5-(7-(9-phenyl-9H-carbazol-2-yl)benzo[1,2,5]thiadiazol-4-yl)thiophene-2-yl)acrylic acid (**SD5**)

Brown Black solid (0.5 g, 80%), MS (MALDI) *m/z*: 554.05 (M<sup>+</sup>), 554.09 (calcd.). FT-IR (KBr): 3437.9 (OH stretch), 3056.9 (=CH stretch), 2214.9 (CN stretch), 1617 (CO stretch), 1503 (C=C aromatic stretch), and 1237.4 cm<sup>-1</sup> (C–O single bond stretch). <sup>1</sup>H NMR (300 MHz, DMSO-*d*<sub>6</sub> δ ppm): 8.40 (d, *J* = 8.07 Hz, 1H), 8.31 (d, *J* = 7.56 Hz, 1H), 8.25–8.20 (m, 2H), 8.15 (s, 1H, olefin), 8.07 (s, 1H, –car), 7.99 (d, *J* = 7.56 Hz, 1H), 7.92 (d, *J* = 7.89 Hz, 1H), 7.82 (d, *J* = 3.3 Hz, 1H), 7.71–7.70 (m, 4H), 7.56–7.53 (m, 1H), 7.48–7.41 (m, 2H), 7.36–7.31 (m, 1H, N-phenyl). Elem. Anal. Calcd. for C<sub>32</sub>H<sub>18</sub>N<sub>4</sub>O<sub>2</sub>S<sub>2</sub>: C, 69.30%; H, 3.27%; N, 10.10%; S, 11.56%. Found: C, 69.06%; H, 3.10%; N, 10.21%; S, 11.73%.

#### 3.6.6. 2-Cyano-3-(5-(7-(9-(4-(2-ethylhexyloxy)phenyl)-9H-carbazol-2-yl)benzo[1,2,5]thiadiazol-4-yl)thiophene-2-yl)acrylic acid (**SD6**)

Black solid (0.1 g, 50% yields), MS (MALDI) *m/z*: 682.2 (M<sup>+</sup>), 682.21 (calcd.), FT-IR (KBr): 3442.1 (OH stretch), 3060.3 (=CH stretch), 2923.9 (–CH stretch), 2216.7 (CN stretch), 1678 (CO stretch), 1625 (C=C alkene stretch), 1560 (C=C aromatic stretch), and 1238.2 cm<sup>-1</sup> (C–O single bond stretch). <sup>1</sup>H NMR (300 MHz, DMSO-*d*<sub>6</sub> δ ppm): 8.40 (d, *J* = 8.2 Hz, 1H), 8.32–8.22 (m, 3H), 8.17 (s, 1H), 8.00 (d, *J* = 7.7 Hz, 2H), 7.93 (d, *J* = 8.3 Hz, 1H), 7.86 (d, *J* = 3.9 Hz, 1H), 7.58 (d, *J* = 8.7 Hz, 2H), 7.47 (t, 1H), 7.36–7.29 (m, 2H), 7.23 (d, *J* = 8.8 Hz, 2H, N-phenyl), 3.97 (d, *J* = 5.5 Hz, 2H, –O–CH<sub>2</sub>–), 1.74–1.72 (m, 1H, –CH–), 1.51–1.32 (m, 8H, –CH<sub>2</sub>–), 0.95–0.82 (m, 6H, –CH<sub>3</sub>–). Elem. Anal. Calcd. for C<sub>40</sub>H<sub>34</sub>N<sub>4</sub>O<sub>3</sub>S<sub>2</sub>: C, 70.36%; H, 5.02%; N, 8.20%; S, 9.39%. Found: C, 70.26%; H, 5.18%; N, 8.31%; S, 9.85%.

## 4. Conclusion

We have designed and synthesized six metal free organic dyes containing N-aryl carbazole derivatives as donor and cyanoacrylic acid as acceptor bridged by benzothiadiazole unit (D-Btz-A) as low band gap chromophores for DSSC. Our approach is unique as it uses an electron-deficient bridge between the push–pull chromophores, leading to *push-pull-pull* architecture that is different from usual *D–π–A*. All the dyes showed broad absorptions in the range of 350–600 nm. In **SD1**, benzothiadiazole acceptor moiety is linked to phenyl-carbazole, showing a conversion efficiency of 1.56%. **SD2** and **SD3** showed maximum conversion efficiencies of 3.29% and 3.8%, respectively, where benzothiadiazole acceptor group is attached to 3-position of N-phenyl/(2-ethylhexyl) carbazole as compared to other dyes. But **SD5** and **SD6** showed low conversion efficiencies, due to the 2-position linkage of benzothiadiazole acceptor group to the N-substituted carbazole. The photophysical, electrochemical, and photovoltaic performances of all six molecules were established, by varying nature and position of substituents on the donor moiety and keeping the acceptor moiety unchanged. The alkoxy substituted dyes showed lower photocurrent values resulting to low power conversion efficiencies. The detailed investigation on the effect of N-(4-phenylalkoxy) substitution on carbazole with other redox couples and co-adsorbents is under progress in our laboratory.

## Acknowledgements

We greatly acknowledge the support of department of chemistry, National University of Singapore for providing facilities and NUS computer centre for high performance computation. AK and LY thanks NUS NanoCore and National University of Singapore for graduate scholarship.

## Appendix A. Supplementary information

Supplementary data related to this article can be found at <http://dx.doi.org/10.1016/j.dyepig.2013.07.002>.

## References

- Chen C-H, Hsu Y-C, Chou H-H, Thomas KRJ, Lin JT, Hsu C-P. Dipolar compounds containing fluorene and a heteroaromatic ring as the conjugating bridge for high-performance dye-sensitized solar cells. *Chem Eur J* 2010;16(10):3184–93.
- O'Regan B, Grätzel M. A low-cost, high-efficiency solar cell based on dye-sensitized colloidal TiO<sub>2</sub> films. *Nature* 1991;353(6346):737–40.
- Saga T. Advances in crystalline silicon solar cell technology for industrial mass production. *NPG Asia Mater* 2010;2(3):96–102.
- Mishra A, Fischer MKR, Bäuerle P. Metal-free organic dyes for dye-sensitized solar cells: from structure: property relationships to design rules. *Angew Chem Int Ed* 2009;48(14):2474–99.
- Grätzel M. Solar energy conversion by dye-sensitized photovoltaic cells. *Inorg Chem* 2005;44(20):6841–51.
- Yanagida M, Yamaguchi T, Kurashige M, Hara K, Katoh R, Sugihara H, et al. Panchromatic sensitization of nanocrystalline TiO<sub>2</sub> with cis-bis(4-carboxy-2-[2'-(4'-carboxypyridyl)]quinoline)bis(thiocyanato-N)ruthenium(II). *Inorg Chem* 2003;42(24):7921–31.
- Hagfeldt A, Boschloo G, Sun L, Klöö L, Pettersson H. Dye-sensitized solar cells. *Chem Rev* 2010;110(11):6595–663.
- Koumura N, Wang Z-S, Mori S, Miyashita M, Suzuki E, Hara K. Alkyl-functionalized organic dyes for efficient molecular photovoltaics. *J Am Chem Soc* 2006;128(44):14256–7.
- Wang H, Zhang X, Gong F, Zhou G, Wang Z-S. Novel ester-functionalized solid-state electrolyte for highly efficient all-solid-state dye-sensitized solar cells. *Adv Mater* 2012;24(1):121–4.
- Kimura M, Nomoto H, Masaki N, Mori S. Dye molecules for simple co-sensitization process: fabrication of mixed-dye-sensitized solar cells. *Angew Chem Int Ed* 2012;51(18):4371–4.
- Grätzel M. Photoelectrochemical cells. *Nature* 2001;414(6861):338–44.
- Hamann TW, Jensen RA, Martinson ABF, Van Ryswyk H, Hupp JT. Advancing beyond current generation dye-sensitized solar cells. *Energy & Environmental Science* 2008;1(1):66–78.
- Wu K-L, Li C-H, Chi Y, Clifford JN, Cabau L, Palomares E, et al. Dye molecular structure device open-circuit voltage correlation in Ru(II) sensitizers with heteroleptic tridentate chelates for dye-sensitized solar cells. *J Am Chem Soc* 2012;134(17):7488–96.
- Goncalves LM, de Zea Bermudez V, Ribeiro HA, Mendes AM. Dye-sensitized solar cells: a safe bet for the future. *Energy & Environmental Science* 2008;1(6):655–67.
- Kim B-G, Chung K, Kim J. Molecular design principle of all-organic dyes for dye-sensitized solar cells. *Chem Eur J* 2013;19(17):5220–30.
- Grätzel M. Recent advances in sensitized mesoscopic solar cells. *Acc Chem Res* 2009;42(11):1788–98.
- Zhang G, Bala H, Cheng Y, Shi D, Lv X, Yu Q, et al. High efficiency and stable dye-sensitized solar cells with an organic chromophore featuring a binary [small pi]-conjugated spacer. *Chem Commun* 2009;16:2198–200.
- Yella A, Lee H-W, Tsao HN, Yi C, Chandiran AK, Nazeeruddin MK, et al. Porphyrin-sensitized solar cells with cobalt (II/III)-based redox electrolyte exceed 12 percent efficiency. *Science* 2011;334(6056):629–34.
- Hara K, Sayama K, Ohga Y, Shinpo A, Suga S, Arakawa H. A coumarin-derivative dye sensitized nanocrystalline TiO<sub>2</sub> solar cell having a high solar-energy conversion efficiency up to 5.6%. *Chem Commun* 2001;6:569–70.
- Hara K, Wang Z-S, Sato T, Furube A, Katoh R, Sugihara H, et al. Oligothiophene-containing coumarin dyes for efficient dye-sensitized solar cells. *J Phys Chem B* 2005;109(32):15476–82.
- Rochford J, Chu D, Hagfeldt A, Galoppini E. Tetrachelate porphyrin chromophores for metal oxide semiconductor sensitization: effect of the spacer length and anchoring group position. *J Am Chem Soc* 2007;129(15):4655–65.
- Reddy PY, Giribabu L, Lyness C, Snaith HJ, Vijaykumar C, Chandrasekharam M, et al. Efficient sensitization of nanocrystalline TiO<sub>2</sub> films by a near-IR-absorbing unsymmetrical zinc phthalocyanine. *Angew Chem Int Ed* 2007;46(3):373–6.
- Dentani T, Kubota Y, Funabiki K, Jin J, Yoshida T, Minoura H, et al. Novel thiophene-conjugated indoline dyes for zinc oxide solar cells. *New J Chem* 2009;33(1):93–101.
- Wang Z-S, Li F-Y, Huang C-H. Highly efficient sensitization of nanocrystalline TiO<sub>2</sub> films with styryl benzothiazolium propylsulfonate. *Chem Commun* 2000;20:2063–4.
- Ooyama Y, Harima Y. Molecular designs and syntheses of organic dyes for dye-sensitized solar cells. *Eur J Org Chem* 2009;2009(18):2903–34.
- Im H, Kim S, Park C, Jang S-H, Kim C-J, Kim K, et al. High performance organic photosensitizers for dye-sensitized solar cells. *Chem Commun* 2010;46(8):1335–7.
- Tang Z-M, Lei T, Jiang K-J, Song Y-L, Pei J. Benzothiadiazole containing D-π-A conjugated compounds for dye-sensitized solar cells: synthesis, properties, and photovoltaic performances. *Chem Asian J* 2010;5(8):1911–7.
- Srinivas K, Kumar CR, Reddy MA, Bhanuprakash K, Rao VJ, Giribabu L. D-π-A organic dyes with carbazole as donor for dye-sensitized solar cells. *Synth Met* 2011;161(1–2):96–105.
- Wang Z-S, Koumura N, Cui Y, Takahashi M, Sekiguchi H, Mori A, et al. Hexylthiophene-functionalized carbazole dyes for efficient molecular photovoltaics: tuning of solar-cell performance by structural modification. *Chem Mater* 2008;20(12):3993–4003.
- Kajiyama S, Uemura Y, Miura H, Hara K, Koumura N. Organic dyes with oligo-n-hexylthiophene for dye-sensitized solar cells: Relation between chemical structure of donor and photovoltaic performance. *Dyes Pigm* 2012;92(3):1250–6.
- Promarak V, Ruchirawat S. Synthesis and properties of N-carbazole end-capped conjugated molecules. *Tetrahedron* 2007;63(7):1602–9.
- Tseng Y-H, Shih P-I, Chien C-H, Dixit AK, Shu C-F, Liu Y-H, et al. Stable organic blue-light-emitting devices prepared from poly[spiro(fluorene-9,9'-xanthene)]. *Macromolecules* 2005;38(24):10055–60.
- Yang J, Jiang C, Zhang Y, Yang R, Yang W, Hou Q, et al. High-efficiency saturated red emitting polymers derived from fluorene and naphthoselenadiazole. *Macromolecules* 2004;37(4):1211–8.
- Huang J, Niu Y, Yang W, Mo Y, Yuan M, Cao Y. Novel electroluminescent polymers derived from carbazole and benzothiadiazole. *Macromolecules* 2002;35(16):6080–2.
- Zhang X-H, Cui Y, Katoh R, Koumura N, Hara K. Organic dyes containing thieno [3,2-b]indole donor for efficient dye-sensitized solar cells. *J Phys Chem C* 2010;114(42):18283–90.
- Zhang X-H, Wang Z-S, Cui Y, Koumura N, Furube A, Hara K. Organic sensitizers based on hexylthiophene-functionalized indolo[3,2-b]carbazole for efficient dye-sensitized solar cells. *J Phys Chem C* 2009;113(30):13409–15.
- Koumura N, Wang Z-S, Miyashita M, Uemura Y, Sekiguchi H, Cui Y, et al. Substituted carbazole dyes for efficient molecular photovoltaics: long electron lifetime and high open circuit voltage performance. *J Mater Chem* 2009;19(27):4829–36.
- Boschloo G, Hagfeldt A. Characteristics of the iodide/triiodide redox mediator in dye-sensitized solar cells. *Acc Chem Res* 2009;42(11):1819–26.
- Velusamy M, Justin Thomas KR, Lin JT, Hsu Y-C, Ho K-C. Organic dyes incorporating low-band-gap chromophores for dye-sensitized solar cells. *Org Lett* 2005;7(10):1899–902.
- Kroeze JE, Hirata N, Koops S, Nazeeruddin MK, Schmidt-Mende L, Grätzel M, et al. Alkyl chain barriers for kinetic optimization in dye-sensitized solar cells. *J Am Chem Soc* 2006;128(50):16376–83.
- Ren X, Jiang S, Cha M, Zhou G, Wang Z-S. Thiophene-bridged double d-π-a dye for efficient dye-sensitized solar cell. *Chem Mater* 2012;24(17):3493–9.
- Lai W-Y, He Q-Y, Chen D-Y, Huang W. Synthesis and characterization of starburst 9-phenylcarbazole/triazatruxene hybrids. *Chem Lett* 2008;37(9):986–7.
- Kim S-K, Lee Y-M, Lee C-J, Lee J-H, Oh S-Y, Park J-W. Synthesis and hole-transporting properties of phenyl-carbazyl derivatives. *Molec Cryst Liq Cryst* 2008;491(1):133–44.
- Keerthi A, Valiyaveetil S. Regioisomers of perylene diimide: synthesis, photophysical, and electrochemical properties. *J Phys Chem B* 2012;116(15):4603–14.
- Frisch MJTGW, Schlegel HB, Scuseria GE, Robb MA, Cheeseman JR, Scalmani G, et al. Gaussian 09, revision A02. Wallingford CT: Gaussian, Inc.; 2009.
- Dennington R, Keith T, Millam J. Semicem Inc Shawnee Mission KS, GaussView, Version 5; 2009.